Local epitaxial growth of CuO films on MgO

Andrei Catana* and Jean-Pierre Locquet
IBM Research Division, Zurich Research Laboratory, 8803 Rüschlikon, Switzerland

Sun M. Paik† and Ivan K. Schuller
Physics Department-0319, University of California, San Diego, La Jolla, California 92039-0319
(Received 30 March 1992)

We have investigated the structure of molecular-beam-epitaxy-grown CuO thin films on MgO substrates using reflection high-energy electron diffraction, x-ray diffraction, and high-resolution electron microscopy (HREM). The results show that CuO(111) planes grow parallel to (001)MgO planes. Three main in-plane epitaxial relations are observed: $[\bar{1}10]$CuO‖[110]MgO, $[0\bar{1}1]$CuO‖[110]MgO, and $[10\bar{1}]$CuO‖[100]MgO. Close to the interface, strains related to the matching conditions imposed by the substrate affect both symmetry and lattice constants of the monoclinic CuO structure. Cross-sectional HREM shows that the exact epitaxial orientation is only partially preserved as the film thickness increases. The loss of in-plane epitaxy is affected by a poor matching of lattice spacings and by misorientations between planes of both crystals, which join at the interface. We investigate the relative orientations between both crystals on the basis of a *mapping technique* developed for the epitaxy of the axial-commensurate system. The results show that all the experimentally observed epitaxial orientations are successfully predicted by this technique.

I. INTRODUCTION

Copper oxide (CuO) is an insulator chemically close to the cuprate superconductors which makes it an interesting candidate as a buffer or interdiffusion layer. It has previously been reported that CuO grows epitaxially on MgO.[1] This may seem surprising in view of the large differences in structure and symmetry between both materials, although lattice-mismatched epitaxy has been known for many years.[2] In this paper we focus on the structure of the CuO/MgO interface using *in situ* reflection high-energy electron diffraction (RHEED), x-ray diffraction, and high-resolution transmission electron microscopy (HREM). CuO grows preferentially with the (111) plane parallel to (001)MgO with three in-plane orientations: $[\bar{1}10]$CuO‖[110]MgO, $[0\bar{1}1]$CuO‖[110]MgO, and $[10\bar{1}]$CuO‖[100]MgO. These local epitaxial orientations are predicted by the *mapping technique*[3] developed for the epitaxy of the axial-commensurate system. In addition, the mapping model predicts two new orientations at relative angle θ (i.e., the angle between $[\bar{1}10]$CuO and [100]MgO) $=-30.45°$ and 14.61°. Lattice misfit of the observed epitaxial orientations ranges from 1% for the $[\bar{1}10]$CuO‖[110]MgO orientation to 9.6% for the $[10\bar{1}]$CuO‖[100]MgO orientation. For the low misfit case ($[\bar{1}10]$CuO‖[110]MgO), the epitaxial orientation is preserved through the whole thickness of the CuO layer, whereas for the large misfit case ($[10\bar{1}]$CuO‖[100]MgO) the exact orientation is lost after deposition of a few monolayers.

II. EXPERIMENT

A description of the experimental details has been reported elsewhere.[1] The CuO layers were prepared in a molecular-beam-epitaxy (MBE) system, with Cu evaporated from a standard effusion cell in an oxygen background pressure generated by an *in situ* rf plasma source which delivers a flow of activated oxygen onto the substrate. Typical deposition conditions are the substrate temperature 675 °C and the background oxygen pressure of 5×10^{-6} Torr. The surface structure is investigated during growth by reflection high-energy electron diffraction (RHEED). After the deposition, the substrate is cooled to room temperature without increasing the pressure. The HREM study was performed in a JEOL-JEM 1020 microscope operating at 200 kV. Thin specimens were prepared for cross-sectional observations along [100] and [110]MgO axes by conventional thinning and ion milling. In order to check the epitaxial orientations, image calculations were performed using the Bloch wave algorithm developed by Stadelmann.[4] The microscope parameters used as input for the calculation are spherical aberration coefficient $=0.5$ mm, spread of focus $=8$ nm, and beam semiconvergence $=0.8$ mrad.

III. RESULTS AND DISCUSSION

A. Crystal structure

CuO has a monoclinic unit cell with the following dimensions: $a_0=4.684$ Å, $b_0=3.425$ Å, $c_0=5.129$ Å, and $\beta=99.47°$. In this structure Cu atoms stack in chains parallel to [110] and $[\bar{1}10]$ which are separated by oxygen planes [Fig. 1(a)]. Each Cu atom is surrounded by a square of oxygens with a Cu-O bond of approximately 1.88 and 1.96 Å, while each oxygen atom is surrounded by a distorted tetrahedron of copper atoms.[5] The CuO(111) plane consists of a two-dimensional rhombic unit cell with the basis of four Cu atoms at (0,0), $(\frac{1}{2}, 0)$, (0,

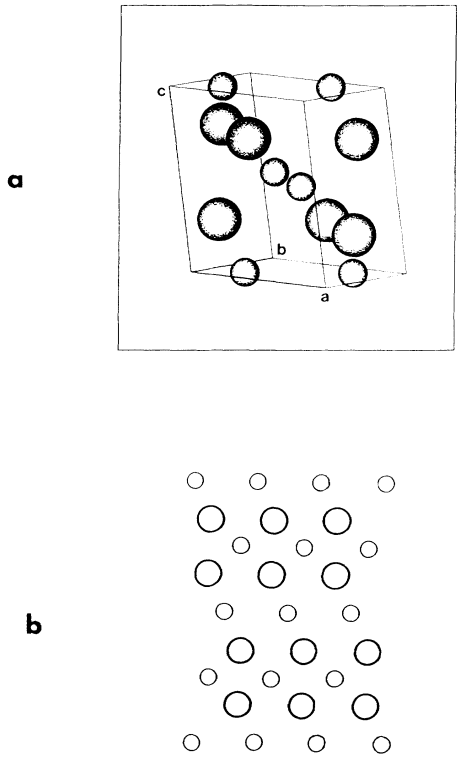

FIG. 1. (a) CuO unit cell: the stacking of Cu atoms (small spheres) in chains parallel to [110] and [$\bar{1}$10] is clearly visible. (b) The CuO(111) plane with the metal atoms represented as small spheres.

$\frac{1}{2}$), and ($\frac{1}{2}$, $\frac{1}{2}$), and four O atoms between the Cu atoms [Fig. 1(b)].

B. Epitaxial orientations

RHEED images recorded during the growth of the CuO film are presented along (a) MgO[110] and (b) MgO[100] orientations in Fig. 2. Along both directions line broadening is observed, indicating that the film is composed of small domains, but the in-plane symmetry is conserved. The in-plane lattice parameter along the [100]MgO direction increases slightly (compared to the MgO spacing) in agreement with an epitaxial [10$\bar{1}$]CuO||[100]MgO orientation and the perpendicular spacing corresponds to the distance between the CuO(111) planes (2.3 Å).

The x-ray-diffraction pattern is shown in Fig. 3. In addition to the substrate peak, only the (111)CuO peak is present. The presence of other peaks under the substrate peak was verified by rocking the substrate a few degrees. This does not prove the epitaxial nature of the film, but indicates a strong (111) texture. The position of the CuO reflection suggest that the (111) spacings (2.34 Å) are slightly larger than the reported bulk value of 2.323 Å.[5]

Transmission electron microscopy (TEM) observations indicate that the CuO layer is polycrystalline with a typical grain size of 20–40 nm, and that the interface and top

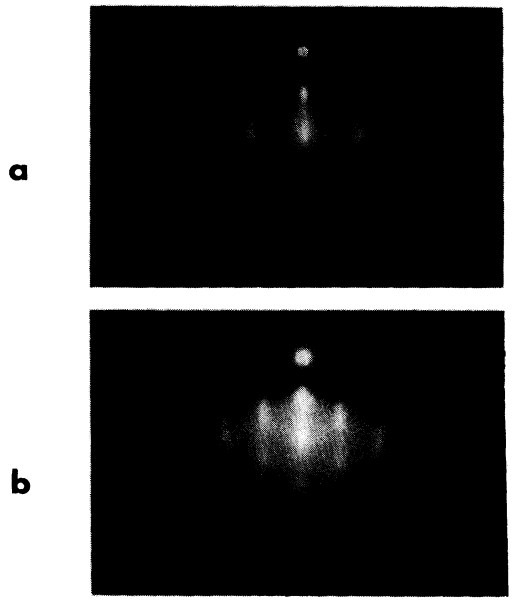

FIG. 2. RHEED images along (a) the [110] and (b) the [100] orientations after deposition of 95-Å CuO.

surface of the film are rough. Selected area diffraction (SAD) patterns and HREM recorded on different domains show that CuO grows preferentially with its close-packed (111) planes parallel to the (001)MgO planes in agreement with x-ray-diffraction measurements. The preferential growth of (111)CuO planes parallel to the (001)MgO planes is presumably related to comparable in-plane atomic densities since the (111)CuO plane provides the closest match (11.49 atoms/nm^2) to the (001)MgO plane (11.72 atoms/nm^2). Consequently, the number of pairwise interactions across the interface reaches a maximum, which in turn lowers the interfacial energy.

In these (111)CuO planes, three orientation relationships have been observed locally: [$\bar{1}$10]CuO||[110]MgO (E_1), [0$\bar{1}$1]CuO||[110]MgO (E_2),

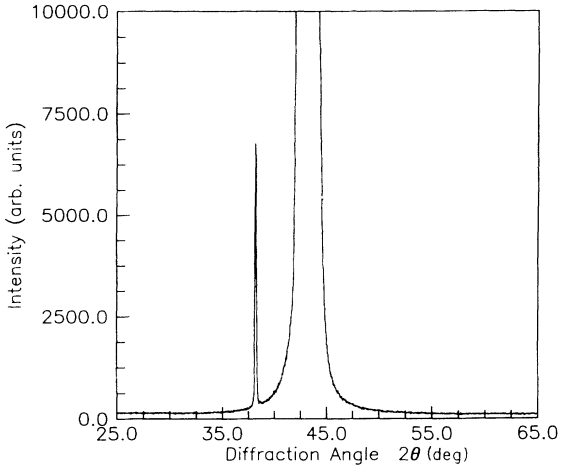

FIG. 3. X-ray diffraction of a 95-Å-thick CuO film on MgO.

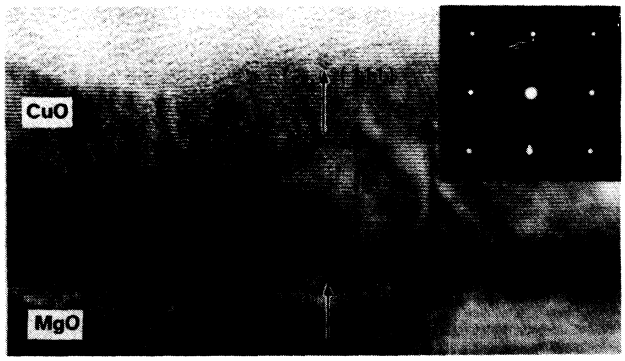

FIG. 4. HREM and SAD (inset) of the CuO/MgO interface showing (111)CuO||(001)MgO. Small domains with [10$\bar{1}$]CuO||[100]MgO are locally observed. Contrast modulations close to the interface indicate the presence of distorted regions.

and [10$\bar{1}$]CuO||[100]MgO (E_3). The HREM micrograph in Fig. 4 shows CuO domains oriented with [10$\bar{1}$]CuO||[100]MgO and (111)CuO||(001)MgO. The corresponding SAD (inset in Fig. 4) proves that the (111)CuO planes are parallel to the (001)MgO planes. Detailed investigation of the image contrast and interplanar spacings at the interface (Fig. 5) indicate that the first 6–10 CuO monolayers grow epitaxially. The growth of these first CuO monolayers is accompanied by strong lattice and angular distortions which partially accommodate

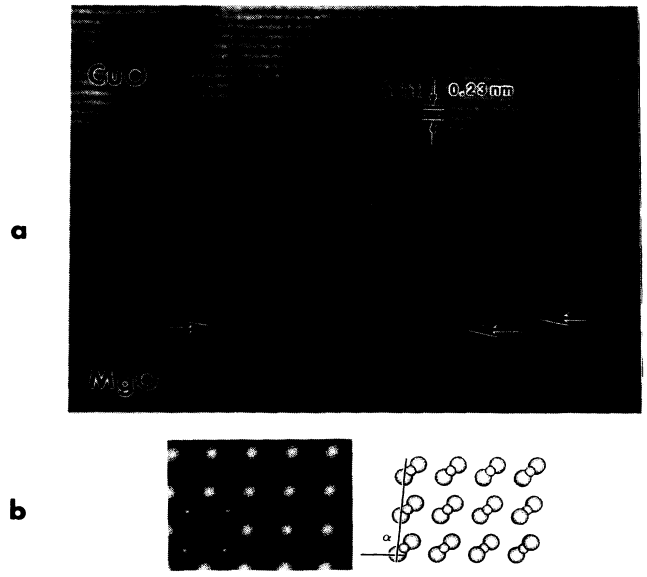

FIG. 5. (a) HREM of an interface region where [10$\bar{1}$]CuO||[100]MgO. The large arrow indicates the MgO/CuO interface. After the first 6–10 CuO layers the epitaxial relation is lost. (b) Corresponding calculated image (defocus =36 nm, sample thickness =6 nm) of CuO and inset of the projected atomic potential. In the inset bright dots represent the Cu positions. Next to the calculation a structural projection is shown (Cu atoms:small spheres).

the 10% lattice mismatch between the (1$\bar{1}$1)CuO and (010)MgO planes at the interface. The angle α between the (111) and (1$\bar{1}$1)CuO planes in this film derived from experimental micrographs is 91°±1°, which is different from the bulk value of 94.8° as indicated by the corresponding calculated image and structural projection [Fig. 5(b)]. The strained epitaxial growth mode of CuO breaks down after a few monolayers and the atomic resolution in the HREM micrograph is lost due to small misorienta-

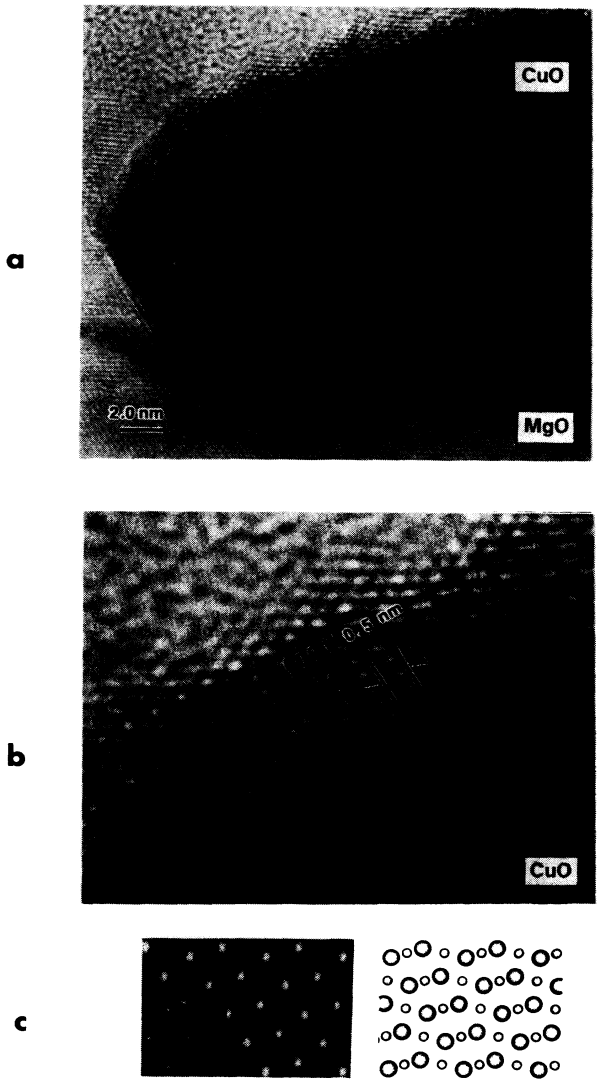

FIG. 6. (a) CuO grain oriented such that [1$\bar{1}$0]CuO||[110]MgO, (111)CuO||(001)MgO. The epitaxial relation is preserved up to the film surface. The surface is undulated as opposed to regions where the exact orientation is lost during growth (for example, Fig. 4). Experimental (b) and calculated (c) high-resolution images of the CuO grain showing the typical contrast modulations parallel to the (002) planes. The inset on the calculated image (defocus =60 nm, sample thickness =8 nm) shows the projection of the atomic potential (bright spots represent Cu atoms). Next to the calculation a structural projection is displayed (Cu atoms: small spheres).

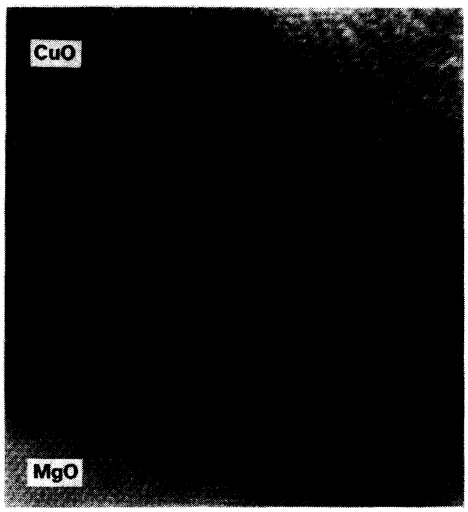

FIG. 7. Adjacent CuO grains oriented with [$\bar{1}$10] and [1$\bar{1}$0] parallel to [110]MgO.

tions with respect to the electron beam axis. Further CuO growth preserves the parallelism between the (111)CuO and (001)MgO planes and ends at the surface with flat domains.

Epitaxial regions where CuO preserves its orientation over the whole thickness have been observed: they correspond to orientation E_1 and are associated with undulated surfaces as shown in Fig. 6. The comparison between the experimental high-resolution micrograph and the corresponding calculated image confirms the epitaxial orientation. In each epitaxial region (E_1, E_2, and E_3), four types of epitaxial domains oriented $\pm 90°$ and 180° with respect to each other have been observed; however, considering the fourfold symmetry of the MgO (001) surface (Fig. 7), they are equivalent.

C. The mapping technique

In this section a theoretical framework is presented which allows us to predict the different relative orientations. The interfacial energy is a sum of the overlayer-substrate (o-s) interaction and the strain energy, and therefore the overlayer film grows in a direction which minimizes this energy. Since the interparticle potentials of these materials are not known, a direct calculation of the interfacial energy is very difficult, if not impossible. However, using the mapping technique that has been developed to study the epitaxy of metallic axial-commensurate systems,[3] the epitaxial orientations of the CuO films on the MgO and their physical properties can be explained. As we pointed out earlier,[3] this method does not require detailed knowledge of the interaction potentials. It utilizes the symmetry of the two lattices and calculates lattice-match/mismatch effects. Other effects that cannot be included in the mapping technique, such as electronic effects, defects, and chemical bonding may also complicate the problem. However, the good agreement with experiment implies that the lattice-match effects are the dominant contribution to the epitaxial orientation in the system.

With the assumption that the o-s interaction potential has the periodicity and symmetry of the substrate surface lattice, the total o-s interaction can be written as

$$V_{\rm os}=\sum_l \sum_m \sum_i^{N_l} \sum_j^{N_m} V^{lm}(\mathbf{r}_i,\mathbf{r}_j)=\sum_{\mathbf{G}} \sum_l V_{\mathbf{G}}^l \sum_i^{N_l} e^{-i\mathbf{G}\cdot\mathbf{r}_i} , \quad (1)$$

where l and m represent different species in the overlayer and the substrate layer, i.e., l = Cu, O and m = Mg, O, respectively, and $\mathbf{r}_i,\mathbf{r}_j$ denote the position of the atoms in their respective layer. N_l, N_m, $\mathbf{G}$, and $V_{\mathbf{G}}^l$ are the number of l atom species in the overlayer, the number of m atoms species in the substrate, the substrate surface reciprocal-lattice vectors, and the Fourier transform of V^{lm}, respectively. Here, the exponential factors $\sum_i^{N_l} \exp[-i\mathbf{G}\cdot\mathbf{r}_i]$ represent the lattice-match/mismatch effects, and the details of interatomic potential are contained in $V_{\mathbf{G}}^l$. For a large system, the summation over i in Eq. (2) can be converted into an integration over the unit cell[3]

$$V_{\rm os}=\sum_{\mathbf{G}} \sum_l V_{\mathbf{G}}^l \frac{1}{\nu_c} \int_{\rm cell} d\mathbf{r}\, f^l(\mathbf{r}) e^{-i\mathbf{G}\cdot\mathbf{r}} e^{-i\mathbf{G}\cdot\mathbf{r}_0} , \quad (2)$$

where ν_c, $f^l(\mathbf{r})$, and $\mathbf{r}_0$ are the surface area of a substrate unit cell, a distribution function when all the overlayer atoms were mapped into the unit cell, and the origin of the overlayer, respectively. Here the term *cell* denotes integration over a unit cell of the substrate surface. In general, the lower $V_{\rm os}$ energy will be obtained when the area covered by $f^l(\mathbf{r})$ is small.

For an incommensurate system, $f^l(\mathbf{r})$ is a uniform distribution.[3,6] The integral yields $\delta_{\mathbf{G},0}$, and the total o-s interaction is $V_{\rm os}=\sum_l V_0^l$. On the other hand, for a perfect lattice-matched system, the distribution $f^l(\mathbf{r})$ becomes a δ function. The total o-s interaction of this system is $V_{\rm os}=\sum_{\mathbf{G}}\sum_l V_{\mathbf{G}}^l \cos[\mathbf{G}\cdot\mathbf{r}_0]$ and will be lowest when $\mathbf{r}_0$ is placed in a minimum.

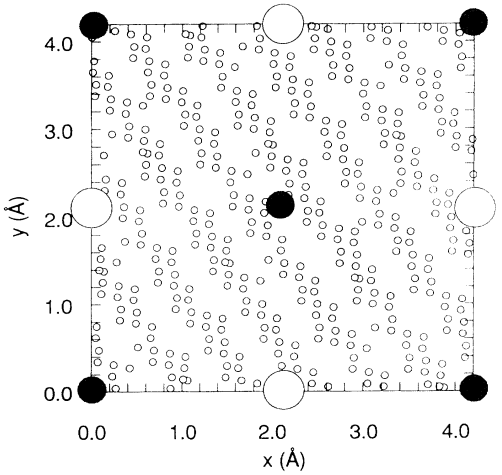

FIG. 8. The mapping pattern $f^l(\mathbf{r})$ of the 21×21×1 CuO(111) unit cell (about 150 Å in linear scale) into MgO(001) unit cell at the relative orientation $\theta=10°$ (the angle between the [$\bar{1}$10]CuO row and [100]MgO).

When overlayer and substrate lattices have completely different symmetries, a perfect lattice match cannot be achieved. The lowest energy configuration in these systems is when the so-called "axial-commensurate matches" occur.[3,7] The $f^l(\mathbf{r})$ consists of a single line for the first-order axial-commensurate match and m equally spaced lines for m-order axial-commensurate matches.

D. Comparison with experiment

We investigate the distribution function $f^l(\mathbf{r})$ as a function of the overlayer surface directions and in-plane relative orientation of the CuO layer with respect to the substrate surface by mapping all the overlayer lattice points into the substrate unit cell. In most cases, $f^l(\mathbf{r})$ is a uniform distribution similar to that in Fig. 8 except at a few relative orientations. At a certain relative orientation $f^l(\mathbf{r})$ is a line distribution (axial-commensurate matches). Here we will concentrate only on the first-order axial-commensurate matches (a single distribution). Considering a few percent lattice distortion, we find five first-order axial-commensurate matches when the CuO(111) plane is parallel to the MgO(001) plane. Three of these matches agree with the experimental observations. We also find two first-order axial-commensurate matches for CuO(010) and CuO(001) planes on MgO(100). These orientations, however, are not observed in the experiments.

Figure 9(a) shows a mapping pattern $f^l(\mathbf{r})$ of a CuO(111) surface of $21\times21\times1$ unit cells (about 150 Å in linear size) into a MgO(001) unit cell at the relative orientation E_1 $[\bar{1}10]$CuO‖[110]MgO and CuO(111)‖MgO(001), and the corresponding lattice-matching configuration is shown in Fig. 9(b). This type of distribution occurs because the distance between two adjacent $[\bar{1}10]$CuO rows ["A" in Fig. 9(b) $=6.0205$ Å] roughly matches a diagonal of the MgO(001) lattice (5.958 Å). (Because of this the axial-commensurate matches are sometimes denoted as "row matching.") When the above two values are exactly the same [referred to as "ideal epitaxial configuration (IEC)"],[3,8] the mapping pattern will be a single line[9] as shown by the dashed line in Fig. 9(a). This orientation has certainly lower V_{os} energy than that of Fig. 8, because all the points here are located either on minima or saddle points whereas many points in Fig. 8 are placed on the potential maxima. Thus the CuO film will grow preferentially in this direction. The lattice misfit $f_A=(A-A_{\mathrm{IEC}})/A$, where A_{IEC} is the distance of A at the IEC[3,7] is about 1%. This misfit should be accommodated by a CuO lattice contraction along the direction perpendicular to $[\bar{1}10]$ (along the axial-commensurate axis) and finite cluster size effects.

In addition to matching arguments, the occurrence of this particular orientation may be favorably influenced by the atomic configurations of the facing interfacial planes. These configurations are displayed in Fig. 10. It turns out that the interfacial planes are both described by unmixed metal and oxygen chains sequentially stacked along $[\bar{1}34]$CuO and [110]MgO. Since the spacings be-

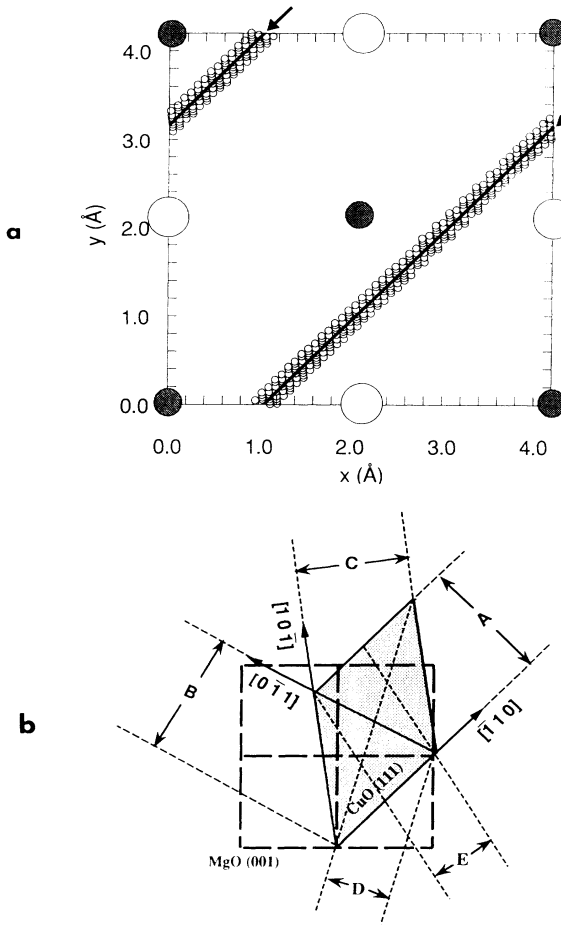

FIG. 9. (a) The mapping pattern $f^l(\mathbf{r})$ of the $21\times21\times1$ CuO(111) unit cell into MgO(001) unit cell at the relative orientation $[\bar{1}10]$CuO‖[110]MgO, CuO(111)‖MgO(001), and (b) the corresponding lattice-match configuration. The bold line in (a), indicated by arrows, is the $f^l(\mathbf{r})$ for the IEC of this orientation. The open and shaded circles in (a) represent oxygen and magnesium atoms, respectively.

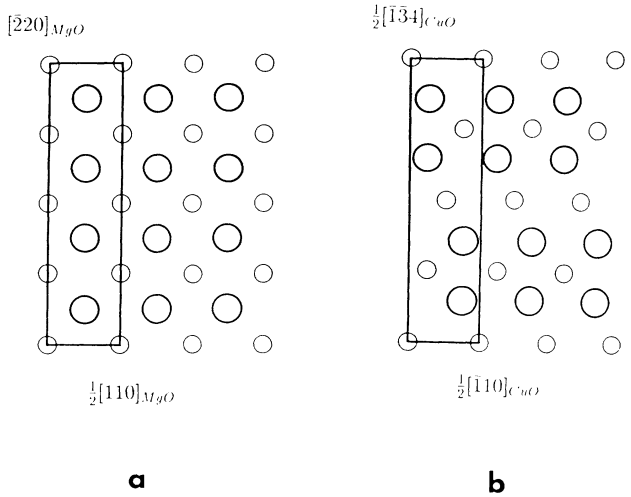

FIG. 10. Atomic configurations in the (001)MgO (a) and (111)CuO (b) planes (metal atoms:small spheres). Superimposed nearly coincident unit cells are indicated in bold.

tween such chains (in particular metallic chains) are almost identical in both crystals, an energetically favorable overlap occurs between unmixed metallic and oxygen rows at the interface. Similar situations have been reported for interfaces between metals and ionic crystals. Fecht and Gleiter[10] successfully explained their results on the basis of a "lock-in" model which associates low-energy boundaries to configurations where close-packed rows of atoms fit into the "valleys" between close-packed rows of atoms belonging to the ionic crystal. At this point it is interesting to note that the epitaxial relationship $[\bar{1}10]$CuO$\|[110]$MgO, CuO(111)$\|$MgO(001) is also predicted by the near-coincidence-site-lattice (NCSL) model[11] (the resulting unit cell of the NCSL is superimposed on the atomic projections in Fig. 10). However, this model fails to predict the two other orientations that have been observed experimentally.

For E_2 $[0\bar{1}1]$CuO$\|[110]$MgO and CuO(111)$\|$MgO(001), a similar mapping pattern as in Fig. 9(a) is obtained except that the distribution is wider. In this case, the length "*B*" in Fig. 9(b) roughly matches the diagonal of the MgO lattice. The lattice misfit ($f_B = -5\%$) of this orientation is larger than the previous orientation and, consequently, the lattice distortion in this orientation will be larger. The CuO lattice will be expanded along the direction perpendicular to the $[0\bar{1}1]$ direction.

The mapping pattern for the axial-commensurate match at relative orientation E_3 $[10\bar{1}]$CuO$\|[100]$MgO and CuO(111)$\|$MgO(001) is shown in Fig. 11. The ideal epitaxial configuration (dashed line in Fig. 11) is obtained when the length "*C*" (which equals 4.661 Å) in Fig. 9(b) matches the lattice constant of the [100]MgO. The misfit in this case is the rather large $f_C = 9.6\%$ but, as shown in the experiment above, about a 10% lattice misfit can be partially accommodated, as has frequently been observed in many metallic systems.[7]

Two other axial-commensurate matches are also found at the relative orientation θ (i.e., the angle between $[\bar{1}10]$CuO and [100]MgO) $= -30.45°$ and $14.61°$ for CuO(111)$\|$MgO(001). Mapping patterns of both matches are similar to that in Fig. 11. The IEC of the orientation $\theta = -30.45°$ ($\theta = 14.61°$) occurs when the length "*D*" ("*E*") match half the diagonal of the MgO(001) lattice. The lattice misfits are $f_D = -6.1\%$ for $\theta = -30.45°$ and $f_E = -1.5\%$ for $\theta = 14.61°$. This theoretical study predicts the two orientations, and there is at present no good reason why they have not been found experimentally. More detailed work is underway to resolve that open question.

Because of the lattice misfits from the IEC's, the CuO film is strained and deformed in order to satisfy the epitaxial relations (the strain energy should still be smaller than the magnitude of the V_{os}). The strain energy increases as the thickness of the CuO layer increases, and eventually reaches a value where the strain energy is too large to be accommodated by the V_{os}. Above this point, the strain energy will be released by the loss of the epitaxial relationship, producing extra grain boundaries, etc. In addition to other factors, the larger misfit produces higher strain energy. Thus, the E_3 $[10\bar{1}]$CuO$\|[110]$MgO epitaxial orientation (the misfit $f_C = 9.6\%$) will lose its epitaxial relationship at a much earlier stage, and the E_1 $[\bar{1}10]$CuO$\|[110]$MgO orientation (the misfit $f_A = 1\%$) is preserved for much thicker layers than the other orientations. As a consequence, the E_1 $[\bar{1}10]$CuO$\|[110]$MgO orientation will dominate the surface of a thick CuO layer.

Within the 10% lattice misfit, we find other first-order axial-commensurate matches, i.e., [001]CuO$\|[100]$MgO and CuO(010)$\|$MgO(001) with 9.6% misfit, and [100]CuO$\|[100]$MgO and CuO(001)$\|$MgO(001) with 10%. Although these orientations may form at a very early cluster stage of the film growth, the observation of these orientations may be difficult because of the large misfit factors (consequently unstable). In addition, lateral interaction between the clusters in these orientations and nearby clusters in more stable orientations (i.e., the $[\bar{1}10]$CuO$\|[110]$MgO orientation) may prevent further growth in these orientations.

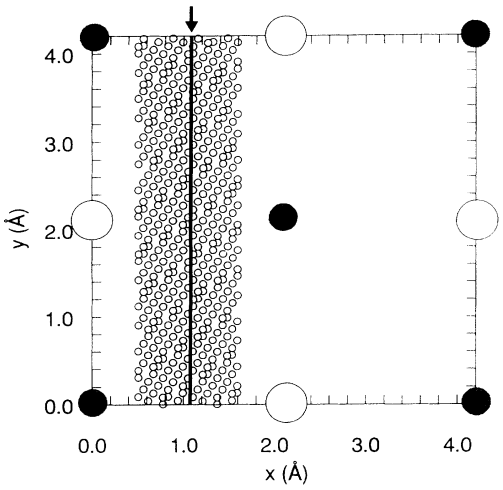

FIG. 11. The same figure as Fig. (9a) for the orientation $[10\bar{1}]$CuO$\|[100]$MgO and CuO(111)$\|$MgO(001).

IV. CONCLUSION

The growth of CuO on MgO is shown to be polycrystalline but strongly textured. Using RHEED, x-ray, and HREM we show that CuO aligns its (111) planes parallel to the (001)MgO planes. Three in-plane orientation relationships have been observed: $[\bar{1}10]$CuO$\|[110]$MgO, $[0\bar{1}1]$CuO$\|[110]$MgO, and $[10\bar{1}]$CuO$\|[100]$MgO. These epitaxial domains do not always preserve their exact orientation up to the film surface. Investigations based on the mapping technique predict all three observed epitaxial orientations. Two new orientations are predicted at the relative orientations $\theta = -30.45°$ and $14.61°$ and we expect experimental confirmation. Since the lattice misfit which characterizes the $[\bar{1}10]$CuO$\|[110]$MgO orientation is the smallest, this orientation is the most stable. Consequently it is preserved for thicker layers as opposed to other orientations, in good agreement with experimental observations.

ACKNOWLEDGMENTS

It is a pleasure to acknowledge valuable support by E. Mächler, R. F. Broom, J. G. Bednorz, and T. Schneider. Work at UCSD was supported by US-DOE Grant No. DE-FG03-87ER-45332 and computer time was provided by the University of California–San Diego Supercomputer Center supported by the US-NSF.

---

*Also at Département de Physique de la Matière Condensée, University of Geneva, 24 quai Ernest-Ansermet, 1211 Geneva, Switzerland.

†Present address: Department of Physics, Kangwon National University, Chunchon, 200-701, Korea.

[1]J.-P. Locquet, J. Less-Common Met. **164-165**, 300 (1990).

[2]See, for example, *Epitaxial Growth,* edited by J. W. Mathews (Academic, New York, 1975); B. A. Joyce, in *Molecular Beam Epitaxy and Heterostructures,* edited by L. L. Chang and K. Ploog, *NATO Advanced Study Institute Series E: Applied Sciences* (Plenum, New York, 1985), No. 87; J. A. Venables, Vacuum **33**, 701 (1983), and references therein. See also, for instance, various articles in MRS Bulletin, edited by R. Messier (Elsevier, New York, 1988), Vol. XIII, No. 11/12.

[3]Sun M. Paik and Ivan K. Schuller, Phys. Rev. Lett. **64**, 1923 (1990); **66**, 395 (E) (1991).

[4]P. Stadelmann, Ultramicroscopy **21**, 131 (1987).

[5]R. W. G. Wyckoff, *Crystal Structures* (Interscience, New York, 1963), Vol. 1.

[6]See, for example, Fig. 8. For an infinite system, the distribution will fill the entire unit cell uniformly.

[7]A. Kobayashi and S. Das Sarma, Phys. Rev. B **35**, 8042 (1987).

[8]J. H. van der Merwe and M. W. H. Braun, Philos. Mag. A **45**, 127 (1978); **45**, 145 (1978); **45**, 159 (1978); L. A. Bruce and H. Jaeger, *ibid.* **38**, 223 (1978); L. W. Bruch and J. A. Venables, Surf. Sci. **148**, 167 (1984).

[9]Because of the lattice periodicity a double line is shown in Fig. 9(a), but this is different from a double line distribution of the second-order axial-commensurate matches.

[10]H. J. Fecht and H. Gleiter, Acta Metall. **33**, 557 (1985).

[11]R. Bonnet and F. Durand, Philos. Mag. **32**, 997 (1975).

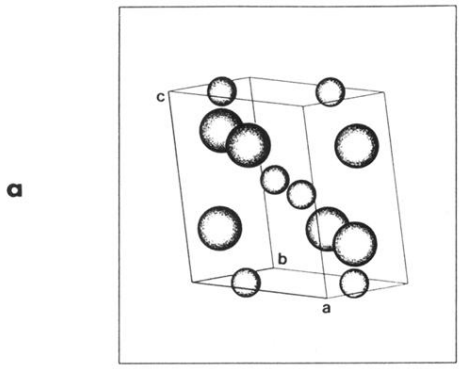

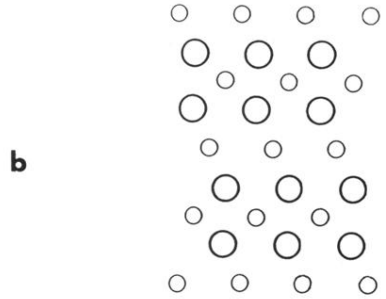

FIG. 1. (a) CuO unit cell: the stacking of Cu atoms (small spheres) in chains parallel to [110] and [$\bar{1}$10] is clearly visible. (b) The CuO(111) plane with the metal atoms represented as small spheres.

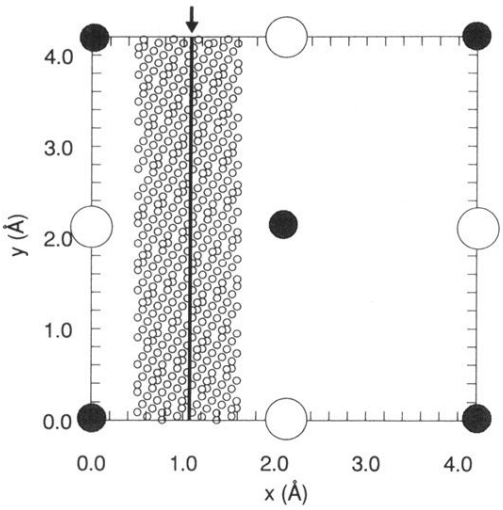

FIG. 11. The same figure as Fig. (9a) for the orientation $[10\bar{1}]$CuO‖[100]MgO and CuO(111)‖MgO(001).

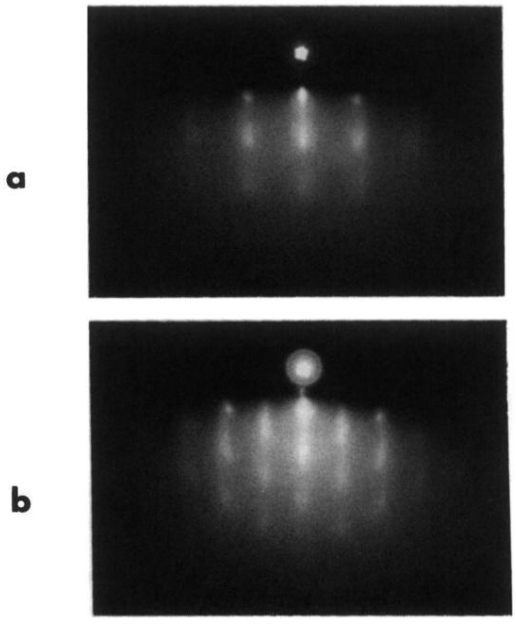

FIG. 2. RHEED images along (a) the [110] and (b) the [100] orientations after deposition of 95-Å CuO.

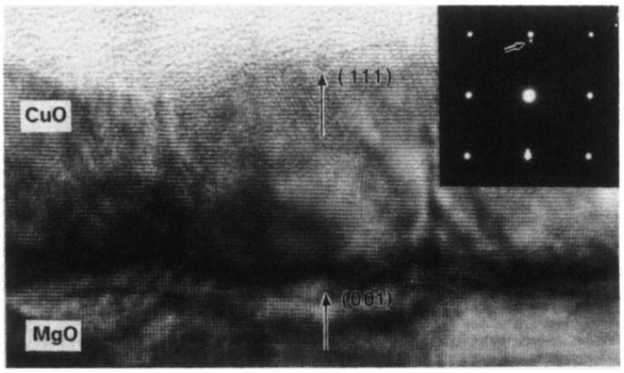

FIG. 4. HREM and SAD (inset) of the CuO/MgO interface showing (111)CuO||(001)MgO. Small domains with $[10\bar{1}]$CuO||[100]MgO are locally observed. Contrast modulations close to the interface indicate the presence of distorted regions.

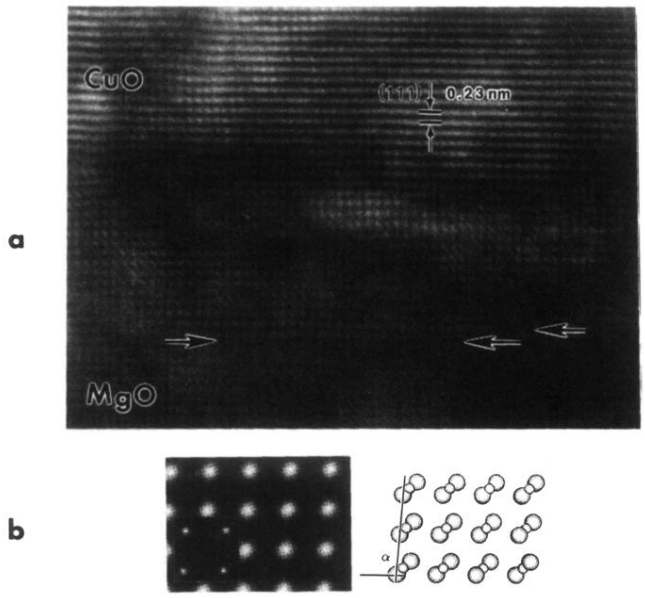

FIG. 5. (a) HREM of an interface region where $[10\bar{1}]$CuO‖[100]MgO. The large arrow indicates the MgO/CuO interface. After the first 6–10 CuO layers the epitaxial relation is lost. (b) Corresponding calculated image (defocus = 36 nm, sample thickness = 6 nm) of CuO and inset of the projected atomic potential. In the inset bright dots represent the Cu positions. Next to the calculation a structural projection is shown (Cu atoms:small spheres).

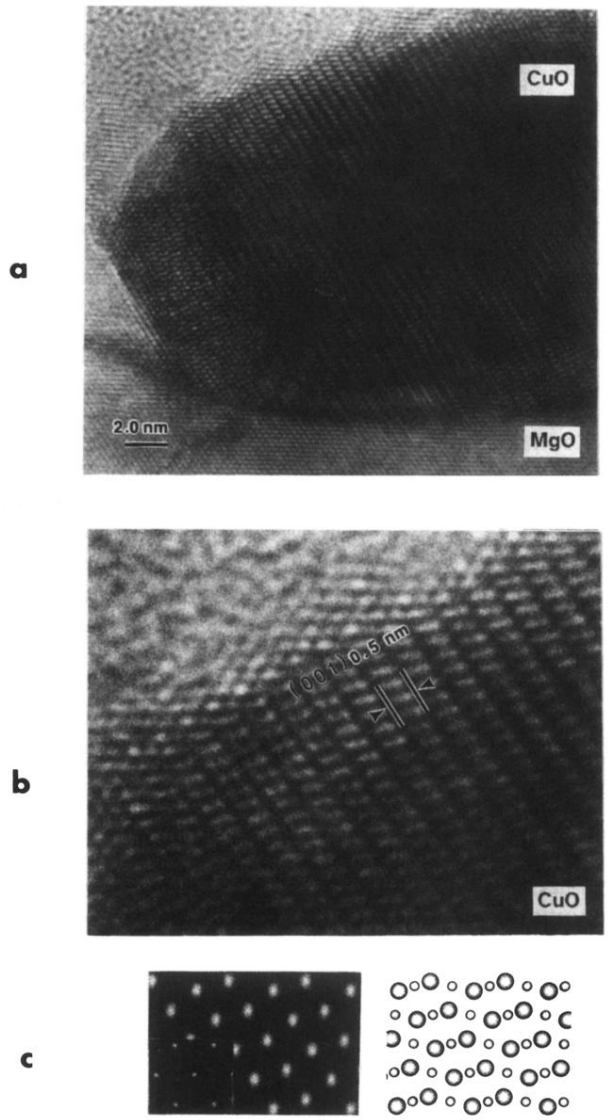

FIG. 6. (a) CuO grain oriented such that $[\bar{1}10]$CuO‖[110]MgO, (111)CuO‖(001)MgO. The epitaxial relation is preserved up to the film surface. The surface is undulated as opposed to regions where the exact orientation is lost during growth (for example, Fig. 4). Experimental (b) and calculated (c) high-resolution images of the CuO grain showing the typical contrast modulations parallel to the (002) planes. The inset on the calculated image (defocus = 60 nm, sample thickness = 8 nm) shows the projection of the atomic potential (bright spots represent Cu atoms). Next to the calculation a structural projection is displayed (Cu atoms: small spheres).

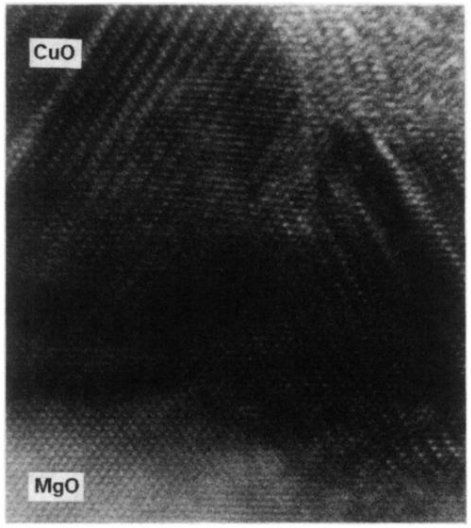

FIG. 7. Adjacent CuO grains oriented with $[\bar{1}10]$ and $[1\bar{1}0]$ parallel to [110]MgO.

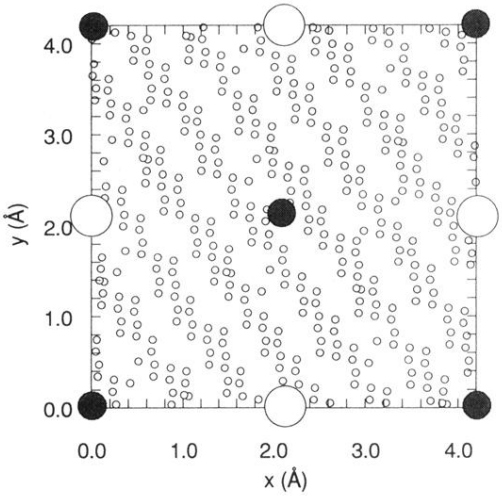

FIG. 8. The mapping pattern $f^{l}(\mathbf{r})$ of the $21\times21\times1$ CuO(111) unit cell (about 150 Å in linear scale) into MgO(001) unit cell at the relative orientation $\theta=10°$ (the angle between the $[\bar{1}10]$CuO row and [100]MgO).

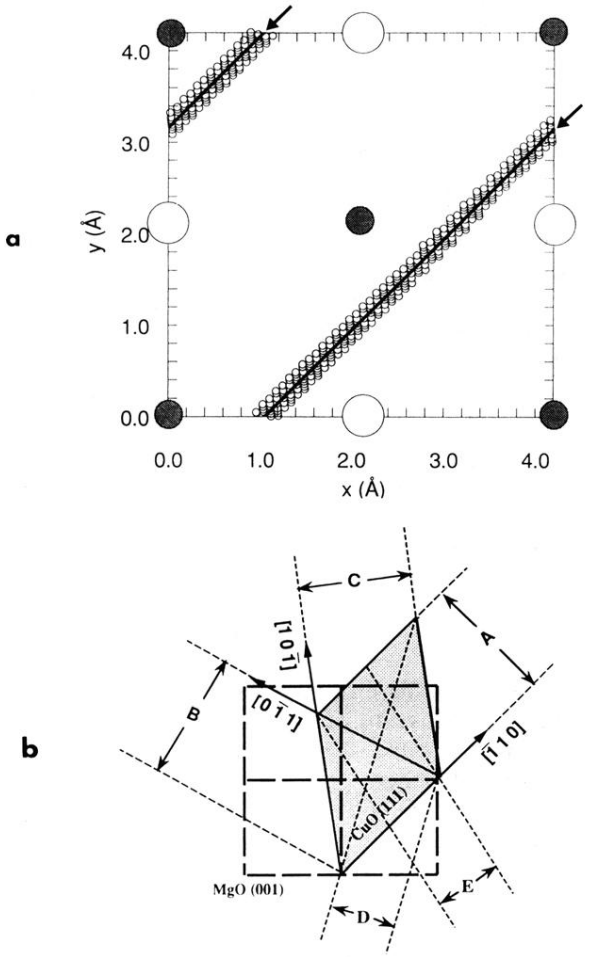

FIG. 9. (a) The mapping pattern $f^{l}(\mathbf{r})$ of the $21\times21\times1$ CuO(111) unit cell into MgO(001) unit cell at the relative orientation $[\bar{1}10]$CuO$\|$[110]MgO, CuO(111)$\|$MgO(001), and (b) the corresponding lattice-match configuration. The bold line in (a), indicated by arrows, is the $f^{l}(\mathbf{r})$ for the IEC of this orientation. The open and shaded circles in (a) represent oxygen and magnesium atoms, respectively.